Carbohydrate Polymers 99 (2014) 638–645

Contents lists available at ScienceDirect

Carbohydrate Polymers

journal homepage: www.elsevier.com/locate/carbpol

Interactions between fluorinated cationic guar gum and surfactants in the dilute and semi-dilute solutions

Chen Wang*, Xiaorui Li, Peizhi Li, Yuhua Niu

Key Laboratory of Auxiliary Chemistry & Technology for Chemical Industry, Ministry of Education, Shaanxi University of Science & Technology, Xi'an 710021, PR China

ARTICLE INFO

Article history:
Received 19 July 2013
Received in revised form 17 August 2013
Accepted 25 August 2013
Available online 2 September 2013

Keywords:
Interactions
Fluorinated cationic guar gum
Surfactants
Hydrophobic micro-domain
Rheological behaviors

ABSTRACT

The interactions between the fluorinated cationic guar gum (FCGG) and ionic surfactants including cetyl trimethyl ammonium bromide (CTAB) and sodium lauryl sulfate (SDS) were studied by light scattering, fluorescence spectroscopy, UV-spectrophotometer, ^{19}F NMR and dynamic rheometer, respectively. The FCGG is prepared with cationic guar gum, isophorone diisocyanate and 2,2,3,4,4,4-hexafluoro-1-butanol. The results show that, with the addition of the surfactants, the stretching degree of the FCGG chains is increased in the FCGG/CTAB solutions, while the dramatical shrinking of FCGG chain, the phase separation and the re-stretched macromolecules appear successively because of the electricity neutralization reaction in the FCGG/SDS system. The mixed hydrophobic domains in all solutions will be reinforced and then dismantled. The solution elasticity shows up the maximum value accordingly. The surfactants can be embedded in the micro-domains and then hinder the fluorinated segmental motions. The interactions between FCGG and SDS are much stronger than those between FCGG and CTAB.

© 2013 Elsevier Ltd. All rights reserved.

1. Introduction

The interactions between water-soluble polymers and surfactants are of growing interest because of their unique associative behavior, special rheological properties and important applications in detergency, mineral separation, pharmaceuticals, rheological control, enhanced oil recovery, paint and coatings, and so forth (Barbieri & Strauss, 1985; Bokias, Hourdet, & Iliopoulos, 2000; Hsu & Strauss, 1987; Kujawa, Ester Goh, Calvet, & Winnik, 2001; Qiu, Lou, Somasundaran, & Pethica, 2002a). These interactive effects are considered to be the result of competition and cooperation between the electrostatic and hydrophobic forces of these complexes (surfactant and polymer). These complexes, besides having important practical applications, also raise some essential questions about the polymer–surfactant interactions that control their behaviors (Deo & Somasundaran, 2005). From the fundamental point of view, understanding the nature of the interactions that lead to the formation of a complex and the physical structure and stability of this complex is fascinating and not clearly established yet (Dibakar & Dinesh, 2001; Qiu, Somasundaran, & Pethica, 2002b).

Previous works about this kind of mixed systems have been dedicated mainly to the weak interactions (e.g., types $P–S^-$ and $P^-–S^-$) or strong interactions (e.g., types $P^+–S^-$ and $P^-–S^+$) (Berglund, Przybycien, & Tilton, 2003; Deo et al., 2003; Goddard & Ananthapadmanabhan, 1993; Kogej, 2003; Kwak, 1998; Sen, Sukul, Dutta, &Bhattacharyya, 2002; Svensson, Picullel, Cabane, & Ilekti, 2002). At present, there is a gradual increase in the studies of the phase behavior and the structural properties in polymer-surfactant solutions (Chu, Yeh, Sokolov, Starodoubtsev, & Khokhlov, 1995; Kogej, Theunissen, & Reynaers, 2002; Okuzaki & Osada, 1995; Zhou, Burger, Yeh, & Chu, 1998). Thus, the interaction between surfactants and polymers has been the subject of active research for the last three decades and it has also been focused on in some of the recent reviews (Hansson, 1998; Kogej, Theunissen, & Reynaers, 2001; Mironov, Starodoubtsev, Khokhlov, Dembo, & Yakunin, 1998).

Guar gum (GG) is a non-ionic, water-soluble, biodegradable and biocompatible heteropolysaccharide. In order to enhance its application scope, the modifications have been reported by several researchers through grafting (Abdel-Halim & Al-Deyab, 2011), derivatization (Trivedi, Kalia, Patel, & Trivedi, 2005) and crosslinking (Barbucci, Pasqui, Favalorob, & Panariello, 2008). Its derivatives with various functional groups hold important potential applications in numerous fields (Ma & Pawlik, 2007). Cationic guar gum (CGG) is a kind of modified guar gum, in which partial hydroxyl groups are replaced by quaternary ammonium groups. The introduction of quaternary ammonium groups imparts cationic characteristics to the gum. Compared with native guar gum, CGG has better solubility and thermal stability in solution and the content of water insoluble substrate is obviously lower than that of native guar gum (Singh, Tiwary, & Kaur, 2010).

* Corresponding author. Tel.: +86 29 86168830; fax: +86 29 86168830.
E-mail address: 277365553@qq.com (C. Wang).

0144-8617/$ – see front matter © 2013 Elsevier Ltd. All rights reserved.
http://dx.doi.org/10.1016/j.carbpol.2013.08.083

In our previous work, we have already incorporated the fluorocarbon chains into CGG and then obtained fluorinated cationic guar gum (FCGG) with excellent solubility and special associative behavior (Wang, Li, Du, Li, & Li, 2013). Since the FCGG will be usually used together with the different kinds of surfactants in its applications, it is very important to gauge the interaction between FCGG and the ionic surfactants. In this work, the FCGG-surfactants (with cetyl trimethyl ammonium bromide or sodium lauryl sulfate) mixed solutions will be studied via the dynamic and static light scattering, fluorescence spectroscopy, UV-spectrophotometer, ^{19}F NMR and dynamic rheometer, respectively. The dilute and semi-dilute solutions are chosen to reveal the FCGG molecular conformations and the influences of surfactants on the interaction between FCGG molecules respectively.

2. Materials and methods

2.1. Materials

The cationic guar gum (CGG) was purchased from Pekin Jiade Biochemistry Co., Ltd. (the weight average molecular weight M_w was approximately 1.0×10^5). Isophorone diisocyanate (IPDI) was purchased from Tianjin Kermel Chemical Reagent Co., Ltd. (Tianjin, China). Dibutyltion dilaurate (T-12) was purchased from Tianjing Hongyan Chemical Reagent Co., Ltd. (Tianjin, China). 2,2,3,4,4,4-Hexafluoro-1-butanol (FH) was purchased from Harbin Xeogia Group Co., Ltd. (Harbin, China). Cetyl trimethyl ammonium bromide (CTAB, c_{cmc} = 0.8 mmol/L), sodium lauryl sulfate (SDS, c_{cmc} = 6.7 mmol/L), acetone, tetrahydrofuran and petroleum ether were from Zhonghai Chemical Industry (Shandong, China). CGG was extracted by acetone for 24 h; Pyrene was recrystallized three times from absolute ethanol. CTAB and SDS were both recrystallized three times from mixed solvents of acetone and absolute ethanol (V:V = 1). Other chemicals were analytical grade and used as received without further purification. Distilled water was used for all experiments.

2.2. Synthesis of FCGG

Firstly, the fluorinated reactive monomer (FAM) based on IPDI and FH was synthesized through solution polymerization. 0.11 mol of IPDI and 50 mL of acetone were charged into a dry vessel fitted with a reflux condenser, a mechanical stirrer, a digital thermometer and a nitrogen gas inlet. The solution of 20 mL of acetone with 0.1 mol of FH was added dropwise into the vessel for 1.0 h. Then the T-12 (0.02 wt.% based on the total reactant mass) was added and the content was stirred for 6.0 h under the state of circulation reflux. After the acetone was removed by distillation, the viscous liquid was obtained and FAM was finally obtained by washing the viscous liquid with petroleum ether three times (100 mL every time).

The CGG was dried to the constant weight in a vacuum at 105 °C for 24 h to remove the free water completely. 8.0 g of the dried CGG and 230 mL of tetrahydrofuran were charged into a dry vessel fitted with the same equipments as shown in the first step. The solution of 20 mL of tetrahydrofuran with different amounts of FAM was added dropwise into the vessel for 1.0 h. Then the T-12 (0.02 wt.% based on the total reactant mass) was added and the content was stirred for another 12.0 h under the state of circulation reflux. The product was extracted from acetone for about 24 h and dried in a vacuum. The fluorinated degree of substitution (DS) was 0.0065 (Wang et al., 2013).

2.3. Preparation of mixed samples

The FCGG-CTAB or FCGG-SDS complex solutions were prepared by slowly adding the appropriate amount of FCGG stock solutions in water to a desired concentration at room temperature under stirring. Then the appropriate amounts of CTAB or SDS were added into the FCGG solutions that had totally been dissolved. Some of the FCGG-SDS mixed solutions became milk-like colloidal systems and a precipitate was obtained in an otherwise milky solution. The only cases of a clear solution were measured.

2.4. Dynamic and static light scattering

The root-mean-square radius of gyration $\langle R_g \rangle$ and the hydrodynamic radius $\langle R_h \rangle$ of the solutions were recorded from CGS-3 compact goniometer system (ALV) with optical maser wavelength at 632 nm at 25 °C. The concentration of the FCGG was 5 mg/L^{-1}(Hong, Zhu, Li, Ngai, Xie, & Wu, 2008). The mixed sample solutions are filtered through a 0.22 μm Durapore membrane before testing.

2.5. Fluorescence spectroscopy (FS)

The fluorescence spectroscopy (FS) of the FCGG-CTAB or FCGG-SDS complex solutions were performed through Fluorophotometer (Cary Eclipse, Agilent) at 25 °C with excitation at 338 nm and with a bandpass slit width of 3.0 nm in a scanning range of 350–550 nm. Polarity parameter (I_1/I_3) of pyrene equal to the ratio of the first to the third emission peak intensities (I_1 = 371 nm, I_3 = 383 nm) was measured. Pyrene was used as fluorescent probe. The solutions for the fluorescence measurements were prepared by first pipetting 0.012 mL of pyrene stock solutions (2.0×10^{-4} mol/L in ethanol). Then, 3.0 mL of polymer solution with a given concentration was added to the flask and also treated by ultrasound for 0.5 h before the FS measurements were carried out.

2.6. Light transmittance

The light transmittance of the solutions is performed on the UV1800 UV-spectrophotometer (SHIMAZU), λ = 440 nm, the test temperature is 25 °C. $T = T_1/T_0 \times 100\%$, where T_1 and T_0 are the light transmittance of sample solutions and reference solution (FCGG solution without SDS), respectively.

2.7. ^{19}F NMR

^{19}F NMR spectra of the FCGG-CTAB or FCGG-SDS complex solutions were analyzed by a NMR spectroscopy (DPX-400 spectrometer, Bruker) at 376.3 MHz. The digital resolution was ±0.01 ppm, with 0.1% in D_2O as solvent.

2.8. Rheological study

The rheological behaviors of FCGGs with different concentrations of CTAB or SDS were performed with the Haake rheometer (RS150L, Therm Haake Co., Germany) equipped with a cone and plate measuring unit. The dynamic measurements were conducted in the range of frequency from 0.01–100 Hz. The test temperature is 25 °C. All the measurements were made within the linear viscoelastic region.

3. Results and discussion

3.1. Shape factor ($\langle R_g \rangle/\langle R_h \rangle$)

$\langle R_g \rangle$ is the root-mean-square radius of gyration of the macromolecules, which is defined as the mean square value of distance (from the quality center of molecular chain to each chain segment) and it is highly related to the actual stretching space of the

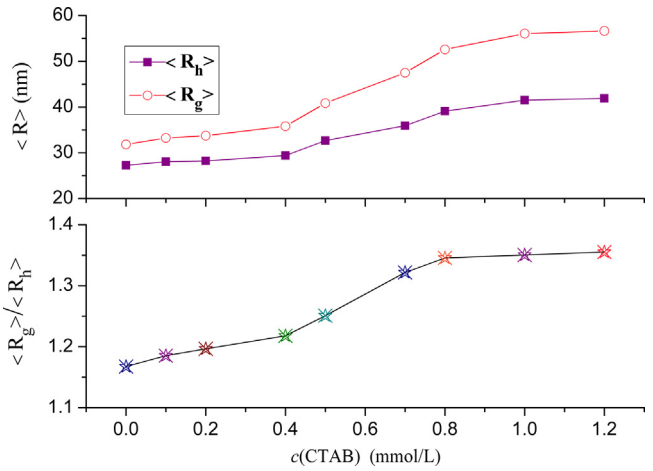

Fig. 1. The $\langle R_g \rangle$, $\langle R_h \rangle$ and the shape factor ($\langle R_g \rangle / \langle R_h \rangle$) of FCGG-CTAB mixed system (c(FCGG) = 5.0 mg/L).

polymer chain. It can be obtained through static LLS from the Eq. (1) as follows.

$$\frac{KC}{R_{VV}(q)} \approx \frac{1}{M_W}\left(1 + \frac{1}{3}\langle R_g^2 \rangle q^2\right) + 2A_2C$$

$$K = 4\pi n^2 \frac{(dn/dC)^2}{N_A \lambda_0^4} \quad (1)$$

$$q = \left(\frac{4\pi n}{\lambda_0}\right) \sin\left(\frac{\theta}{2}\right)$$

where $R_{vv}(q)$, N_A, dn/dC, n, λ_0 and A_2 is Rayleigh ratio, the Avogadro number, the specific refractive index increment, the solvent refractive index, the wavelength of the laser light in a vacuum and the second virial coefficient, respectively. At the same time, one thing to be noted is that the FCGG solution is so dilute ($C \to 0$) in this part and then the term $2A_2C$ in Eq. (1) can be dropped in the extrapolation. It can be gotten from the angular dependence of the excess absolute scattering intensity (Rayleigh ratio $R_{vv}(q)$).

The hydrodynamic radius ($\langle R_h \rangle$) is the equivalent radius of the sphere that has the same translational diffusion coefficient of the measured macromolecules. It can be obtained through dynamic LLS.

The shape factor ($\langle R_g \rangle / \langle R_h \rangle$) is always used for studying the macromolecular conformation and can clearly reflect the density of the chain segment and the polydispersity of the system (Hong et al., 2008). The bigger value of $\langle R_g \rangle / \langle R_h \rangle$ indicates the more stretching macromolecules in the mixed solution system.

3.1.1. FCGG/CTAB complexation in solution

It is obvious that the loose intra-molecular associating structures will be formed when the FCGG molecule coils itself due to the hydrophobic groups in the molecules. As shown in Fig. 1, the $\langle R_g \rangle$, $\langle R_h \rangle$ and the shape factor ($\langle R_g \rangle / \langle R_h \rangle$) are slightly increased with the increase of CTAB concentration before c(CTAB) reaches 0.4 mmol/L. The smaller amounts of CTAB will strengthen the original hydrophobic associating micro-domains (intra-molecules) and the "mixed micelles" will be formed. Although the volume of the mixed micelle is almost the same, the positive charges in the FCGG molecule and CTAB will be repelled each other, which lead to the mild extension of macromolecules.

Then, the $\langle R_g \rangle$, $\langle R_h \rangle$ and the shape factor ($\langle R_g \rangle / \langle R_h \rangle$) present the obvious increasing trend and finally approach a constant value when CTAB is unceasingly added. The change depicts that the addition of CTAB can surely influence the intra-polymeric interactions of the hydrophobic side chains. When CTAB concentration is higher,

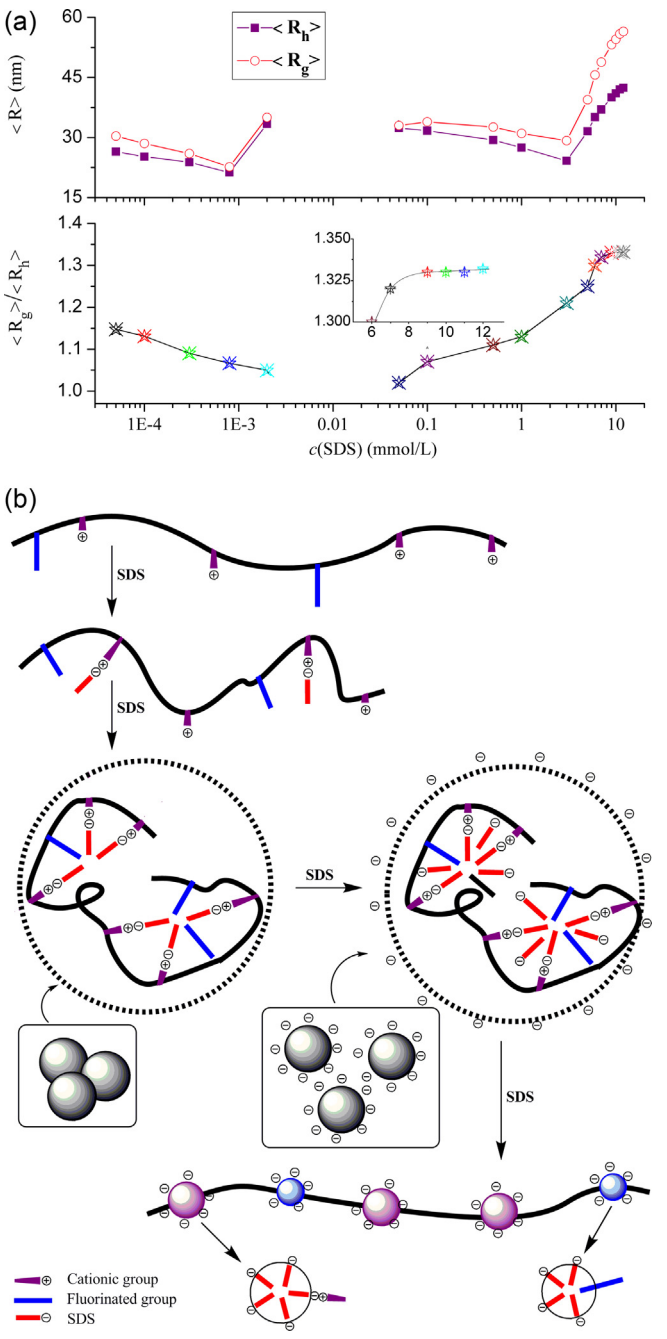

Fig. 2. (a) The $\langle R_g \rangle$, $\langle R_h \rangle$ and the shape factor ($\langle R_g \rangle / \langle R_h \rangle$) of FCGG-SDS mixed system (c(FCGG) = 5.0 mg/L) and (b) the schematic process of FCGG-SDS mixed system (c(FCGG) = 5.0 mg/L) as a increasing amount of the SDS concentration.

intra-molecular association of the polymer is partly shielded and raveled. As a result, there appear lots of new mixed micelles, in which the content of fluorinated groups is very lower and even there is a single fluorinated chain. During the process, the raveled polymer coils become relatively stretched. At the same time, the positive charges are increased rapidly in the mixed system and the extension degree of the macromolecules is improved significantly under the mutual repulsion of charges on the mixed micelles.

3.1.2. FCGG/SDS complexation in solution

The effects of SDS on the properties of the FCGG solution are totally different. When the SDS is added into the FCGG solution, it can be combined with the quaternary ammonium group

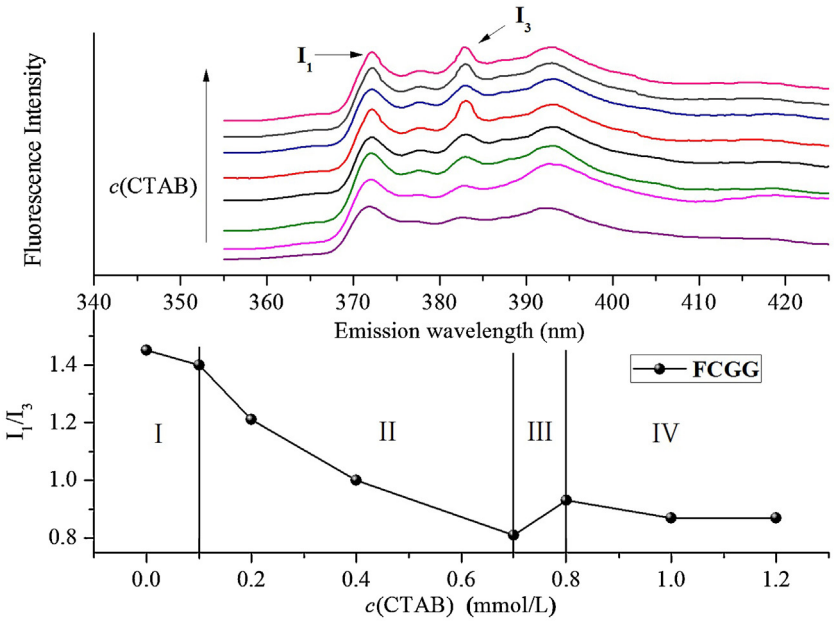

Fig. 3. The fluorescence spectra and I_1/I_3 ratio of FCGG-CTAB mixed system (c(FCGG) = 2.0 g/L).

by ionic bond. These can be regarded as the increase of the hydrophobic groups in FCGG. Hence, the hydrophobicity of the polymer are increased and trace amounts of precipitate will appear when the charges in FCGG molecules are neutralized by the opposite charges in the SDS (in this full neutralized state, the c(SDS) is 4.7×10^{-3} mmol/L). The results are consistent with Dubin (Dubin & Oteri, 1983). However, with the continuous addition of SDS in the separated solution, it is surprised that the homogeneous phase reappears. This process is clearly reflected in Fig. 2(a).

The intra-molecular associative effect is mainly existed in the dilute solution. With the increase of SDS concentration, $\langle R_g \rangle$, $\langle R_h \rangle$ and shape factor ($\langle R_g \rangle / \langle R_h \rangle$) present declining trends. The possible reason is that the increase of "ionic-bonding hydrophobic groups" will enhance the intra-molecular associations of FCGG macromolecules, and thus the macromolecular chains are coiled and contracted (Li, Dubin, Havel, Edwards, & Dautzenberg, 1995). Until the major positive charges in the FCGG are neutralized, the solution takes the form of phase separation. After that, the excess amount of negative charges in the SDS molecule can make the aggregates repelled each other and the $\langle R \rangle$ is increased significantly. The hydrophobic domains will be full of SDS; the FCGG molecules are stretched and take the form of "pearl necklace" by the charge repulsions. The schematic process is shown in Fig. 2(b).

3.2. Fluorescence spectroscopy

The fluorescence probe can reveal the hydrophobic associative property of hydrophobically associating polymer system at the molecule level. The value of I_1/I_3 measured in the fluorescence spectra is equal to the ratio of the first to the third emission peak intensities (I_1 = 371 nm, I_3 = 383 nm) of pyrene. This value is the so-called polarity parameter, which is strongly dependent on the polarity around pyrene probe. The stronger the polarity of microenvironment around the pyrene probe, the higher the value of I_1/I_3 (Ren, Gao, Lu, Liu, & Tong, 2006). For example, the value of I_1/I_3 is 1.87 when the pyrene is in the pure water and it is 0.58 in the nonpolar cyclohexane.

3.2.1. FCGG/CTAB complexation in solution

Fig. 3 shows the fluorescence spectra and the I_1/I_3 values of pyrene for solutions containing 2.0 g/L FCGG as a function of the CTAB concentration.

In the absence of CTAB, the value of I_1/I_3 is 1.45 when the concentration of FCGG solution is 2.0 g/L and is lower than that in a purely aqueous environment (1.87). It indicates that there is already some self-assembly property in FCGG solutions without CTAB. However, if the hydrophobic micro-domains are full of fluorinated groups, this value should be very small, even less than 0.58 (in the cyclohexane). While it is reasonable that the value is 1.45 because the hydrophobic micro-domains are loose and a small amount of water molecules are infiltrated into the loose domains. Finally, the polarity of the microenvironment is only enhanced slightly.

There are four regimes in the $I_1/I_3 \sim c$(CTAB) curve with the addition of CATB. At regime I in Fig. 3, the fluorescence ratio for I_1/I_3 is slightly decreased to 1.40. With the addition of CTAB, the mixed micelles are formed and then the micro-domains is reinforced. Accordingly, the water molecules are gradually squeezed out from the domains. Hence, the polarity of the microenvironment around the probe presents declining slightly. In the regime II, the micro-domains will be persistently strengthened and the polarity is decreased remarkably, which leads to the sharp decline of the I_1/I_3 value. However, learned from regime III, the I_1/I_3 value is increased, which presents that the mixed micelles are taken apart. The content of the strong nonpolar fluorinated chain is decreased along with the increase of the hydrocarbon chain in the micro-domains, and the polarity of the microenvironment is enhanced slightly. At the final regime, the I_1/I_3 ratio is fairly constant with the average values of 0.90. It indicates that the each domain is comprised of the fluorinated chain (or chains) and hydrocarbon chains with constant contents, and the polarity remains the same. As a result, the value of I_1/I_3 appears fairly unchanged as well.

3.2.2. FCGG/SDS complexation in solution

Since there are strong electric neutralizations in the FCGG/SDS mixed system and the phase separation is easily formed. Therefore, the accuracy of the results will be highly affected. In the study,

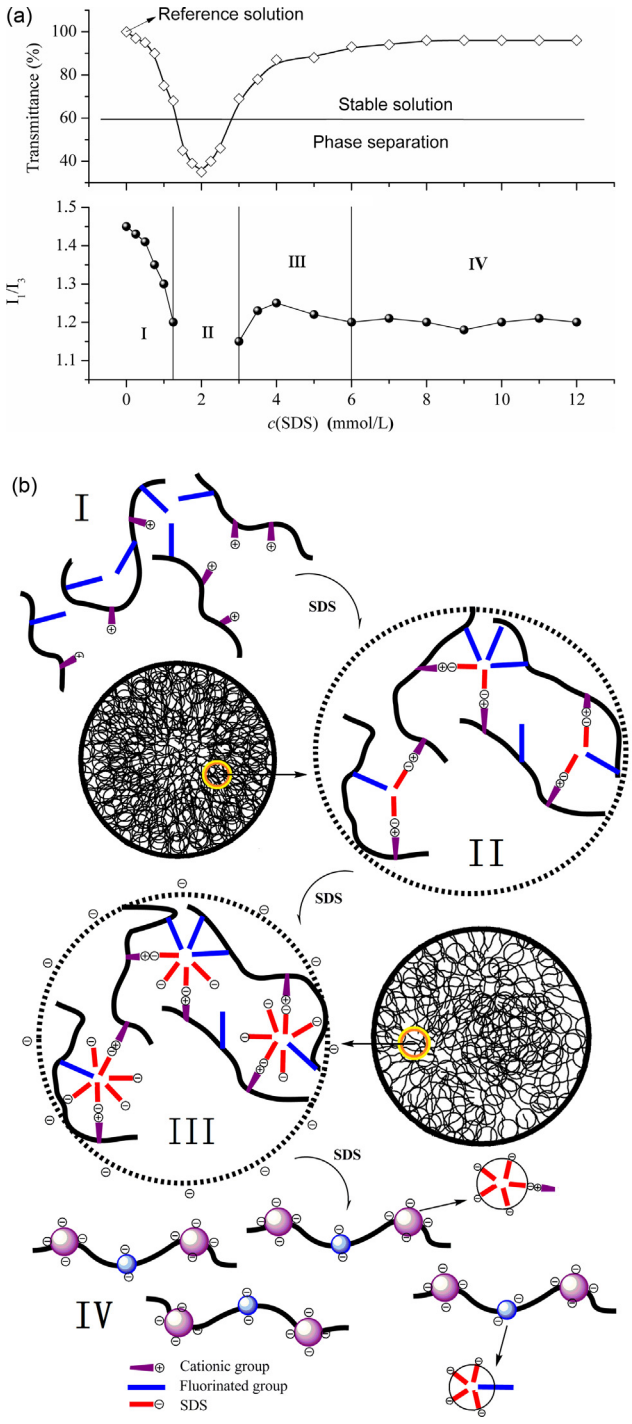

Fig. 4. (a) The light transmittance and I_1/I_3 ratio of FCGG-SDS mixed system (c(FCGG) = 2.0 g/L) and (b) the schematic process of FCGG-SDS mixed system (c(FCGG) = 2.0 g/L) as a increasing amount of the SDS concentration.

we identify the FCGG solution as the blank solution (or reference solution). At the same time, when the light transmittance of the test solution is less than 60%, the solution has been identified as phase separation and then its tests of fluorescence spectra do not be carried out. The light transmittance and I_1/I_3 ratio of sample solutions are clearly illustrated in Fig. 4(a).

The change of the $I_1/I_3 \sim$ c(SDS) curve in the semi-dilute FCGG solution can be also divided into four regimes depicted in Fig. 4(a). Regime I shows the decline of the transmittance and the I_1/I_3 of the solution. The possible reason is that the hydrophilic quaternary ammonium groups in the FCGG can be combined with hydrophilic anionic group in the SDS. It can be regarded as the increase of the hydrophobic groups. Hence, the hydrophobicity of the system will be increased and the inter-molecular associations will be enhanced. These hydrophobic groups assemble together and then the hydrophobic micro-domains are formed.

When the charges in FCGG are gradually neutralized by the opposite charges in SDS, amounts of precipitate (or aggregates) will appear and the transmittance of the system is decreased sharply. At this time, the phase separation is defined. The *c*(SDS) is theoretically calculated as 1.9 mmol/L in this semi-dilute state when the positive charges in FCGG are fully neutralized by the opposite charges in SDS. In the Regime II, the I_1/I_3 value is not presented due to the phase separation.

But in the Regime III, the exceeded SDS will make the macromolecules possessing negative charges and then the macromolecules are stretched by the repelling forces in the three-dimensional network structures. The homogeneous phase reappears when the concentration of SDS is exceeding 3.0 mmol/L. During the addition of SDS, the distances among the macromolecules are increased and the mixed micelles become loose. The water molecules will be infiltrated into the loose domains. At the same time, the hydrophobic groups in SDS are embedded in the mixed micelles, which make the micelles became tight. With the effects of both sides of SDS, the I_1/I_3 value is presented a slight increasing and then decreasing trend accordingly.

In the Regime IV, the solution has already been stable indicated by the steady transmittance values and the I_1/I_3 value is roughly constant. According to the addition of SDS, the increasing amount of SDS and the decreasing amount of the stronger non-polar fluorinated groups in the mixed micelles will take place simultaneously. The former will enhance the value but the latter will lower the value. After all, the content of fluorinated groups in the mixed micelles is very low and its effect is slight. As a result, the I_1/I_3 will basically remain unchanged around a constant value. The effect of SDS on the structure of the FCGG-SDS mixed solutions is schematically shown in Fig. 4(b).

3.3. ^{19}F NMR

Nuclear magnetic resonance (NMR) spectrum is an effective means to analysize the microscopic structural and structural evolutions of the mixed solution between polymer and surfactants (Gharibi, Javadian, Sohrabi, & Behjatmanesh, 2005). It is essentially a kind of absorption spectrum that can indicate the interactive information between FCGG and surfactants in the absence of the probe. The ^{19}F NMR is used in this section because it can clearly and simply testify the interaction of the micro-domains that intermingled via different hydrophobic groups.

3.3.1. FCGG/CTAB complexation in solution

The influence of CTAB content on its interaction with fluorinated chain segment in the FCGG is showed in Fig. 5.

As shown in ^{19}F NMR spectrum of FCGG, it is known that there are three different chemical environments of fluorine atoms in FCGG molecules. Due to the effects of Van der Waals force and coupling effect, the double peaks of $-CF_3$ groups appear in the low-field range (near −68.02 ppm) and the peaks of $-CF_2$ groups appear at near −109.21 ppm. The peaks of CHF appear in the high-field range (−205.12 ppm) without effect of van der Waals force. The results of ^{19}F NMR confirm that the FAM is effectively introduced into FCGG. Compared with the spectra of FCGG, all of the characteristic absorption peaks of the mixed solution with CTAB widen and flatten. Also, they move toward the low field slightly.

With the addition of CTAB, the mixed micelles can form in FCGG solutions. Small amounts of CTAB are able to reinforce the

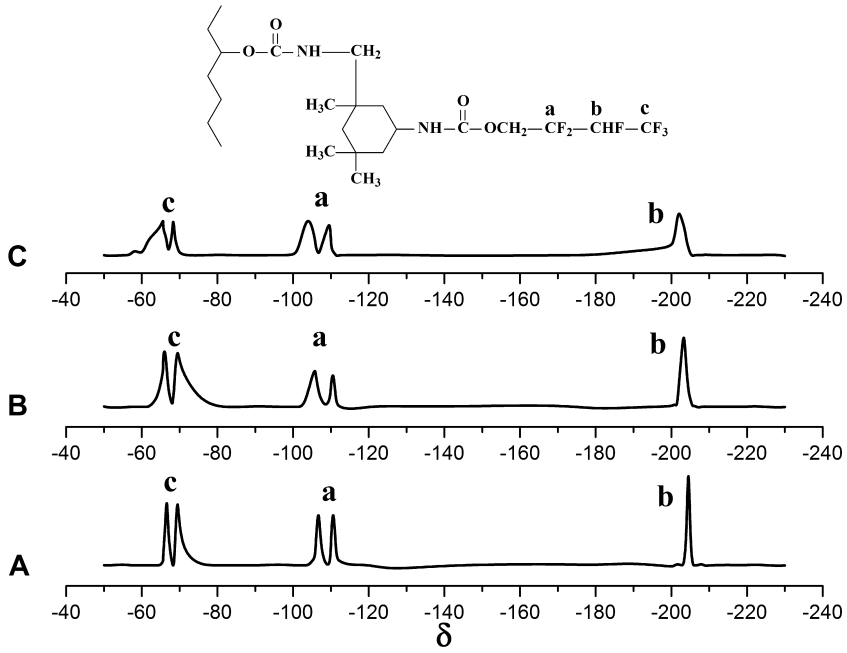

Fig. 5. The ^{19}F NMR spectra of FCGG-CTAB mixed system (A: 2.0 g/L of FCGG; B: 2.0 g/L of FCGG + 0.10 mmL/L of CTAB; C: 2.0 g/L of FCGG + 0.80 mmL/L of CTAB).

aggregates that will hinder the motion of fluorinated chains. This will lead to the wide and flat absorption peaks of C–F. Although the aggregate is dismantled when large amounts of CTAB are added, the single fluorinated chain-centered mixed micelles will form stably. The motion resistance of the fluorinated chain increases and its absorption peak becomes wider and flater.

3.3.2. FCGG/SDS complexation in solution

The cationic charges are neutralized by anionic ones when SDS is added to the FCGG solution. Then, both of the charge density and the hydrophilcity of the macromolecules is decreased, the aggregation degree of the macromolecules is increased. It is worth noting that the phase separation will turn up if the aggregation degree is too large with much addition of SDS. So the original solutions will precipitate. But the homogeneous phase will reappear when the SDS is continued to be added into the solutions. The ^{19}F NMR spectra of the FCGG-SDS system shown in Fig. 6.

Compared with the spectrum of FCGG, the characteristic absorption peaks of the mixed solution also widen and flatten. Moreover, they move toward the low field slightly. However, the changing degree is greater than that of the FCGG-CTAB system. When the more SDS is continued to be add into the system (the homogeneous phase reappears when the concentration of SDS is exceeding 3.0 mmol/L), this changing phenomenon of the characteristic absorption peaks is more obvious, even the individual peak almost disappears.

The reason that the influence of SDS on the absorption peak in the system can be attributed to the following two points: (1) the charge in the SDS can be neutralized with that in the FCGG and thus the ion pair forms, which leads to more “hydrophobic groups”; (2)

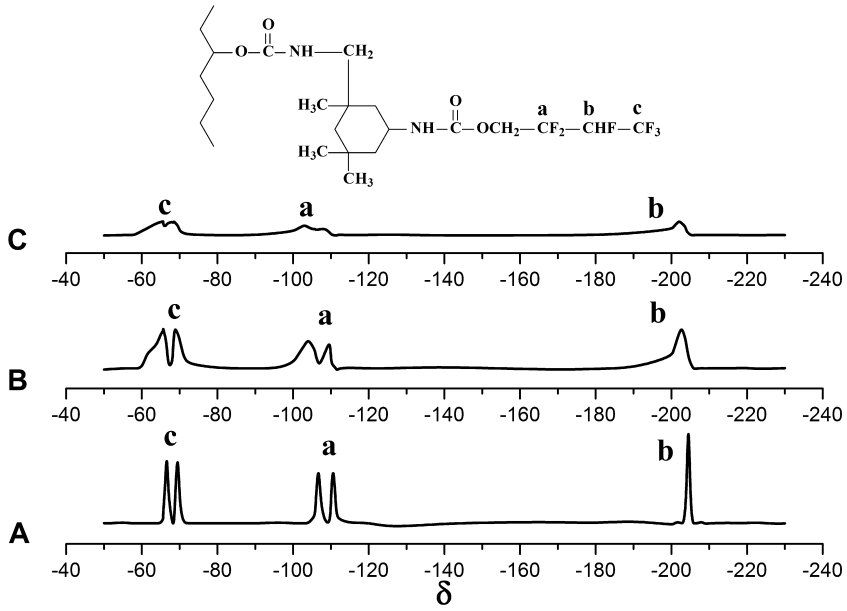

Fig. 6. The ^{19}F NMR spectra of FCGG-SDS mixed system (A: 2.0 g/L of FCGG; B: 2.0 g/L of FCGG + 0.50 mmL/L of SDS; C: 2.0 g/L of FCGG + 8.0 mmL/L of SDS).

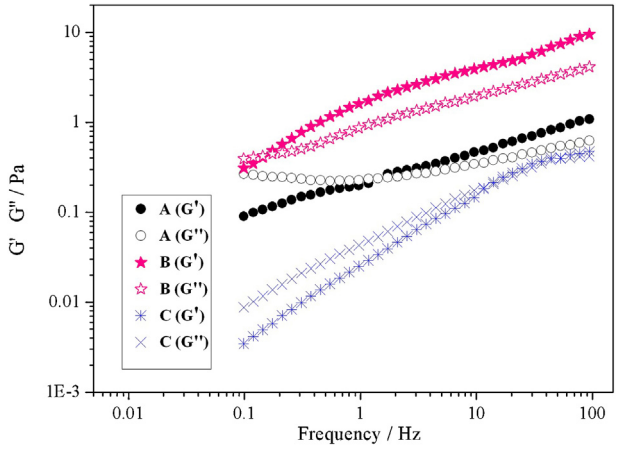

Fig. 7. The storage modulus (G') and loss modulus (G'') of FCGG-CTAB mixed system via frequency (A: 5.0 g/L of FCGG; B: 5.0 g/L of FCGG + 0.20 mmL/L of CTAB; C: 5.0 g/L of FCGG + 1.0 mmL/L of CTAB).

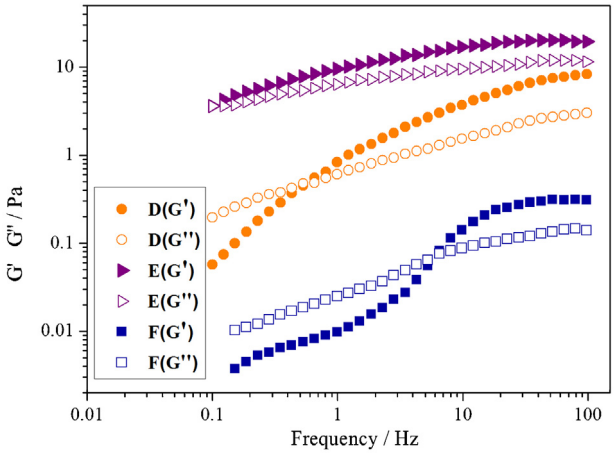

Fig. 8. The storage modulus (G') and loss modulus (G'') of FCGG-SDS mixed system via frequency (A: 5.0 g/L of FCGG+ 1.0 mmL/L of SDS; B: 5.0 g/L of FCGG + 3.0 mmL/L of SDS; C: 5.0 g/L of FCGG + 10.0 mmL/L of SDS).

the charges on macromolecular chain reduce, and the molecular chains coil and shrink. The above two reasons can greatly enhance the aggregate. This makes the motion resistance of the fluorinated chain segment increased, and the absorption peak changes wide, flat, and moves to low field slightly.

With the continuous increase of the SDS, the aggregation will keep on being reinforced. Although the aggregate is dismantled when large amounts of SDS are added, the new, stable and single fluorinated chain-centered mixed micelles will form. As a result, the motion of the fluorinated chain segment will be hindered. So it will be reflected in ^{19}F NMR spectra that the absorption peak becomes wider and smoother, even almost disappears.

3.4. Dynamic moduli

3.4.1. FCGG/CTAB complexation in solution

Similarly, the viscoelastic behaviors of the surfactants-FCGG system will be strongly affected by the self-assemble behaviors of two kinds of the molecules. The dynamic moduli of the system have been performed in the linear viscoelastic region. Fig. 7 describes the storage modulus (G') and the loss modulus (G'') of the FCGG solution with different content of CTAB.

With the 0.2 mmol/L of CTAB in the FCGG solution, both moduli are enhanced and the relaxation spectra are shifted to the relative lower frequencies. This illustrates the importance of the elastic part formed in the mixed system. However, when the content of CTAB is 1.0 mmol/L, it is not found that the G' of the system is larger than G'' at the measured range of frequencies. The viscidity property is more than the elasticity property of this mixed system. In the case of maxwellian behavior, a characteristic relaxation time τ_c can be estimated from the frequency (ω_c) corresponding to the crossing point G_c ($G'(\omega) = G''(\omega)$; $\tau_c = 1/\omega_c$). The τ_c of FCGG solution and its mixed system with 0.2 mmol/L of CTAB is 0.67 s and 6.67 s, respectively. But it decreases to less than 0.01 s of the FCGG solution with 1.0 mmol/L of CTAB. This obvious changed τ_c indicates that a small amount of CTAB can enforce the physically cross-linking net structures and build the viscoelasticity up. Meanwhile, the exceeded amount of CTAB (above its CMC) will dismantle the mixed micelles, dispossess the viscoelasticity and present the viscidity property of the solution. The observed change of the relaxation time indicates an augmentation of the association life-time between fluorinated groups and moderate amount of CTAB.

3.4.2. FCGG/SDS complexation in solution

Considering the phase separation during the addition process of SDS, the concentrations of SDS in the phase separation are avoided in this section. The three characteristic concentrations of SDS on both sides of the phase separation are chosen to study their influences on the moduli of the FCGG-SDS mixed solution, as shown in Fig. 8. With the increase of SDS concentration before the phase separation appears, both moduli are increased a lot and the relaxation spectra are shifted to the lower frequencies. The elastic part is formed in the mixed solution due to the increase of the associating effects via the more "ionic-bonding hydrophobic groups" as said before. This will be depicted by the τ_c and it is increased to 1.82 s when the c(SDS) is 1.0 mmol/L. It is found that the G' is larger than G'' at the measured range of frequencies as the c(SDS) is 3.0 mmol/L. This mixed system shows the elasticity property clearly. When the c(SDS) is 10.0 mmol/L in the FCGG solution, the τ_c is decreased sharply to 0.16 s. The declined τ_c with high SDS concentration shows that the exceeded SDS dissembles the mixed micelles formed by three kinds of hydrophobic groups (fluorinated groups, ionic-bonding hydrophobic groups and SDS) and the viscoelasticity of the mixed system is decreased. This proves that there is surely a decline of the association life-time among three kinds of hydrophobic groups.

4. Conclusion

Here we have investigated how the ionic surfactants influences the conformation and the morphology of the mixed hydrophobic micro-domains formed by the fluorinated cationic guar gum (FCGG) with surfactants in the both dilute and semi-dilute solutions, respectively. Cetyl trimethyl ammonium bromide (CTAB) and sodium lauryl sulfate (SDS) are chosen as the representatives of the different kinds of the ionic surfactants. Because of having the same kinds of the charges, CTAB makes the FCGG chains stretched in dilute solution. In the semi-dilute solutions, the mixed hydrophobic micro-domains are reinforced and then dismantled when the content of CTAB is increased. The effects of SDS on the properties of the FCGG solution are totally different from those of CTAB. After the charges in FCGG are gradually neutralized by the opposite charges in SDS, the new hydrophobic groups are formed and the hydrophobility of the FCGG is increased. As a result, the phenomena of the dramatical shrinking of FCGG chain, the phase separation and the re-stretched macromolecules appear successively in the dilute solution. Of course, the similar change regulation appears in the semi-dilute solutions. It is noted that the difference is rather the enhanced inter-molecular hydrophobical micro-domains than the dramatical shrinking of FCGG chain. The surfactants can be indeed embedded in the mixed micelles and the interactive effect between

the FCGG and SDS (different charges) is much stronger than that between the FCGG and CTAB (same charges).

Acknowledgements

We would like to express our great thanks to the Agricultural science and technology innovation projects of Shaanxi province of China (2012NKC02-09), Shaanxi province science and technology research and development program of China (2013KJXX-77), National Natural Science Foundation of China (21204046) for the financial supports.

References

Abdel-Halim, E. S., & Al-Deyab, S. S. (2011). Hydrogel from crosslinked polyacrylamide/guar gum graft copolymer for sorption of hexavalent chromium ion. *Carbohydrate Polymers*, *86*, 1306–1312.

Barbieri, B. W., & Strauss, U. P. (1985). Effect of alkyl group size on the cooperativity in conformational transitions of hydrophobic polyacids. *Macromolecules*, *18*, 411–414.

Barbucci, R., Pasqui, D., Favalorob, R., & Panariello, G. (2008). A thixotropic hydrogel from chemically cross-linked guar gum: Synthesis, characterization and rheological behaviour. *Carbohydrate Research*, *343*, 3058–3065.

Berglund, K. D., Przybycien, T. M., & Tilton, R. D. (2003). Coadsorption of sodium dodecyl sulfate with hydrophobically modified nonionic cellulose polymers. 1. Role of polymer hydrophobic modification. *Langmuir*, *19*, 2705–2713.

Bokias, G., Hourdet, D., & Iliopoulos, I. (2000). Positively charged amphiphilic polymers based on poly(N-isopropylacrylamide): Phase behavior and shear-induced thickening in aqueous solution. *Macromolecules*, *33*, 2929–2935.

Chu, B., Yeh, F., Sokolov, E. L., Starodoubtsev, S. G., & Khokhlov, A. R. (1995). Interaction of slightly cross-linked gels of poly(diallyldimethylammonium chloride) with surfactants. *Macromolecules*, *28*, 8447–8449.

Deo, P., Jockusch, S., Ottaviani, M. F., Moscatelli, A., Turro, N. J., & Somasundaran, P. (2003). Interactions of hydrophobically modified polyelectrolytes with surfactants of the same charge. *Langmuir*, *19*, 10747–10752.

Deo, P., & Somasundaran, P. (2005). Interactions of hydrophobically modified polyelectrolytes with nonionic surfactants. *Langmuir*, *21*, 3950–3956.

Dibakar, D., & Dinesh, O. S. (2001). Stability of sodium dodecyl sulfate micelles in the presence of a range of water-soluble polymers: A pressure-jump study. *Journal of Physical Chemistry B*, *105*, 7133–7138.

Dubin, P. L., & Oteri, R. (1983). Association of polyelectrolytes with oppositely charged mixed micelles. *Journal of Colloid and Interface Science*, *95*, 453–461.

Gharibi, H., Javadian, S., Sohrabi, B., & Behjatmanesh, R. (2005). Investigation of interaction parmeters in mixed micelle using pulsed field gradient NMR Spectroscopy. *Journal of Colloid and Interface Science*, *285*, 351–359.

Goddard, E. D., & Ananthapadmanabhan, K. P. (1993). *The interactions of surfactants with polymers and proteins*. Boca Raton, FL: CRC Press.

Hansson, P. (1998). Surfactant self-assembly in polyelectrolyte gels: Aggregation numbers and their relation to the gel collapse and the appearance of ordered structures in the NaPA/C12TAB system. *Langmuir*, *14*, 4059–4064.

Hong, L., Zhu, F., Li, J., Ngai, T., Xie, Z., & Wu, C. (2008). Folding of long multiblock copolymer (pi-b-ps-b-pi)n chains prepared by the self-assembly assisted polypolymerization (SAAP) in cyclohexane. *Macromolecules*, *41*, 2219–2227.

Hsu, J.-L., & Strauss, U. P. (1987). Intramolecular micelles in a copolymer of maleic anhydride and hexyl vinyl ether: Determination of aggregation number by luminescence quenching. *Journal of Physical Chemistry B*, *91*, 6238–6241.

Kogej, K. (2003). Study of the effect of polyion charge density on structural properties of complexes between poly(acrylic acid) and alkylpyridinium surfactants. *Journal of Physical Chemistry B*, *107*, 8003–8010.

Kogej, K., Theunissen, E., & Reynaers, H. (2001). Formation of organized structures in systems containing alkylpyridinium surfactants and sodium poly(styrenesulfonate). *Acta Chimica Slovenica*, *48*, 353–362.

Kogej, K., Theunissen, E., & Reynaers, H. (2002). Effect of polyion charge density on the morphology of nanostructures in polyelectrolyte–surfactant complexes. *Langmuir*, *18*, 8799–8805.

Kujawa, P., Ester Goh, C. C., Calvet, D., & Winnik, F. M. (2001). Do fluorocarbon hydrocarbon, and polycyclic aromatic groups intermingle? Solution properties of pyrene-labeled bis(fluorocarbon/hydrocarbon)-modified poly(N-isopropylacrylamide). *Macromolecules*, *34*, 6387–6395.

Kwak, J. C. T. (1998). *Polymer–surfactant systems*. New York: Marcel Dekker.

Li, Y. J., Dubin, P. L., Havel, H. A., Edwards, S. L., & Dautzenberg, H. (1995). Electrophoretic light scattering, dynamic light scattering, and turbidimetry studies of the effect of polymer concentration on complex formation between polyelectrolyte and oppositely charged mixed micelles. *Macromolecules*, *28*, 3098–3102.

Ma, X. D., & Pawlik, M. (2007). Intrinsic viscosities and Huggins constants of guar gum in alkali metal chloride solutions. *Carbohydrate Polymers*, *70*, 15–24.

Mironov, A. V., Starodoubtsev, S. G., Khokhlov, A. R., Dembo, A. T., & Yakunin, A. N. (1998). Ordered nonstoichiometric polymer gel–surfactant complexes in aqueous medium with high ionic strength. *Macromolecules*, *31*, 7698.

Okuzaki, H., & Osada, Y. (1995). Ordered-aggregate formation by surfactant-charged gel interaction. *Macromolecules*, *28*, 380–382.

Qiu, Q., Lou, A., Somasundaran, P., & Pethica, B. A. (2002). Intramolecular Association of poly(maleic acid/octyl vinyl ether) in aqueous solution. *Langmuir*, *18*, 5921–5926.

Qiu, Q., Somasundaran, P., & Pethica, B. A. (2002). Hydrophobic complexation of poly(vinyl caprolactam) with sodium dodecyl sulfate and dodecyltrimethylammonium bromide in solution. *Langmuir*, *18*, 3482–3486.

Ren, B. Y., Gao, Y. M., Lu, L., Liu, X. X., & Tong, Z. (2006). Aggregates of alginates binding with surfactants of single and twin alkyl chains in aqueous solutions: Fluorescence and dynamic light scattering studies. *Carbohydrate Polymers*, *66*, 266–273.

Sen, S., Sukul, D., Dutta, P., & Bhattacharyya, K. (2002). Solvation dynamics in aqueous polymer solution and in polymer–surfactant aggregate. *Journal of Physical Chemistry B*, *106*, 3763–3769.

Singh, M., Tiwary, A. K., & Kaur, G. (2010). Investigations on interpolymer complexes of cationic guar gum and xanthan gum for formulation of bioadhesive films. *Research in Pharmaceutical Sciences*, *5*, 79–87.

Svensson, A., Picullel, L., Cabane, B., & Ilekti, P. (2002). A new approach to the phase behavior of oppositely charged polymers and surfactants. *Journal of Physical Chemistry B*, *106*, 1013–1018.

Trivedi, J. H., Kalia, K., Patel, N. K., & Trivedi, H. C. (2005). Ceric-induced grafting of acrylonitrile onto sodium salt of partially carboxymethylated guar gum. *Carbohydrate Polymers*, *60*, 117–125.

Wang, C., Li, X. R., Du, B., Li, P. Z., & Li, H. B. (2013). Associating and rheological behaviors of fluorinated cationic guar gum in aqueous solutions. *Carbohydrate Polymers*, *95*, 637–643.

Zhou, S., Burger, C., Yeh, F., & Chu, B. (1998). Nanostructures of polyelectrolyte gel–surfactant complexes. *Journal of Polymer Science Part B: Polymer Physics*, *37*, 2165–2172.